J. Fluid Mech. (1989), *vol.* 199, *pp.* 217–236
Printed in Great Britain

The effect of a weak vertical magnetic field on the buoyancy-driven boundary-layer flow past a vertical heated wall

By OLIVER S. KERR AND A. A. WHEELER
School of Mathematics, University of Bristol, Bristol, BS8 1TW, UK

(Received 24 February 1988)

In this paper we investigate the effect of a weak vertical magnetic field on the boundary-layer flow of an electrically conducting fluid past a vertical heated wall. We derive similarity solutions for the flow and temperature and show that the flow is composed of three regions: an inner region where the flow is a regular perturbation of the classical boundary-layer flow due to a heated semi-infinite vertical plate; an inviscid outer region where fluid is entrained from downwards towards the plate; and beyond this a quiescent region, separated from the outer region by a free shear layer. Thus the effect of the magnetic field is to inhibit the entrainment of fluid across the magnetic field lines in the whole region and confine it to an outer boundary layer.

1. Introduction

In this paper we consider the effect of a constant magnetic field parallel to a heated vertical wall. The initial motivation for this work was an investigation of the effect of an axial magnetic field on the crucible wall boundary layers that occur in the magnetic Czochralski crystal growth technique. An analysis of this situation has already been conducted by Hjellming & Walker (1987) but in the limit of large magnetic interaction number, in which case the nonlinear inertia terms may be neglected. Such a large value of the magnetic interaction number is not always obtained in practice. The approach adopted here is to consider the situation when the magnetic field is weak; however the equations are fully nonlinear and we have to make several simplifying assumptions in order to make progress. As we are principally concerned with the effect of the magnetic field on the buoyancy-driven flows in the crucible we focus our attention on the more fundamental problem of the flow past a heated vertical flat wall in the presence of a uniform vertical magnetic field.

The heated vertical flat plate with a uniform far-field temperature in the absence of a magnetic field was first considered by Pohlhausen (1921) who developed the classical similarity solution to the boundary-layer equations. There have been various extensions of this work to include magnetohydrodynamic effects. It has been extended to include a transverse magnetic field by, for example, Sparrow & Cess (1961) and Lykoudis (1962). The latter considers a uniform field, whereas the former deals with the case of a field with variation of $x^{-\frac{1}{4}}$, where x is the distance along the plate. Wilks (1976) provided a numerical solution in the case when the horizontal magnetic field is uniform. Gray (1977) investigated the effect of a transverse field on a plume above a heated line source. Other theoretical work which considers a vertical magnetic field is limited to Soward (1969) who is concerned with the interaction of the field with a rising plume above a point or line heat source. Another example where the magnetic field is almost parallel to the predominant direction of the flow was studied by Riley (1976), who considered the case of a parallel magnetic field on the Blasius boundary layer.

The situation that we consider here, of a heated vertical plate in the presence of a parallel vertical magnetic field, has not received attention although experiments on the effect of a vertical magnetic field on the flow in a rectangular container with a heated sidewall have been carried out by Seki, Kawamura & Sanokawa (1979) who also conducted some numerical calculations. A reason why this problem has not been considered may well be because a superficial consideration of this situation would indicate that the flow in the boundary layer, which is almost parallel to the magnetic field, would therefore be virtually unaffected by the Lorenz force. Here we analyse this situation for a small magnetic field using similarity solutions and show that although the standard boundary-layer solution of Pohlhausen (1921) provides the leading-order approximation when the magnetic field is weak, it leads to an infinite pressure difference across the boundary layer. This is because the transverse pressure gradient is unable to entrain the fluid across the magnetic field lines; this is considered in detail in §2. To overcome this difficulty we show that a more complicated boundary-layer structure exists. In §3 we find that there is an inner layer where the flow is represented at leading order by the standard boundary-layer solution. This flow is perturbed by the weak magnetic field. The inner-layer solution breaks down in the far field and indicates the existence of an inviscid outer layer. This is considered in §4, where we demonstrate that, owing to the singular nature of the differential equation for the similarity solution in this region, the flow must involve a discontinuity in the velocity at a finite distance from the plate. Beyond this free shear layer the fluid is quiescent. The presence of the magnetic field does not allow the fluid entrained by the hot rising flow in the inner layer to be supplied from the far field with a predominantly horizontal velocity. Instead the fluid is supplied from the outer region with a predominantly downward flow. In §5 we complete the matching process between the inner and outer layers as well as derive expressions for the Nusselt number. Finally in §6 we discuss the effect of viscosity on the free shear layer.

2. Discussion

Here we are concerned with the behaviour of an electrically conducting fluid which is heated from an isothermal vertical sidewall in the presence of a weak vertical magnetic field. The configuration is shown in figure 1. We assume that the magnetic Reynolds number of the system is negligible. Hence we can ignore the effect of the fluid flow on the magnetic field and so take the magnetic field to be fixed. We adopt the Boussinesq approximation; thus the governing equations are

$$u\frac{\partial u}{\partial x}+v\frac{\partial u}{\partial y} = -\frac{1}{\rho}\frac{\partial p}{\partial x}+g\alpha(T-T_\infty)+\nu\nabla^2 u, \tag{2.1a}$$

$$u\frac{\partial v}{\partial x}+v\frac{\partial v}{\partial y} = -\frac{1}{\rho}\frac{\partial p}{\partial y}-\frac{\sigma B^2}{\rho}v+\nu\nabla^2 v, \tag{2.1b}$$

$$\frac{\partial u}{\partial x}+\frac{\partial v}{\partial y} = 0, \quad u\frac{\partial T}{\partial x}+v\frac{\partial T}{\partial y} = \kappa\nabla^2 T, \tag{2.1c,d}$$

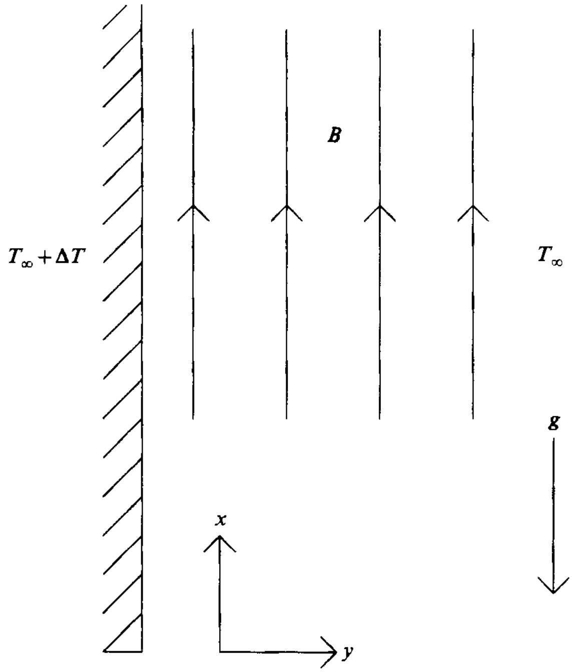

FIGURE 1. Configuration of the flow under consideration. A fluid of temperature T_∞ is heated at a vertical wall to temperature $T_\infty + \Delta T$ in the presence of a weak vertical magnetic field, B. The x-coordinate measures the distance from the bottom of the wall, and y is the horizontal distance from the wall.

where the x- and y-components of the velocity are u and v respectively, p is the pressure and T the temperature. The physical constants are ρ the density, ν the kinematic viscosity, κ the thermal diffusivity, g gravity, α the coefficient of thermal expansion, B the magnetic inductance, and σ the electrical conductivity. The boundary conditions on the flow and temperature are

$$\left.\begin{array}{c} u=0, \quad v=0, \quad T=T_\infty+\Delta T \quad \text{at} \quad y=0, \\ u, v \rightarrow 0, \quad T \rightarrow T_\infty \quad \text{as} \quad y \rightarrow \infty. \end{array}\right\} \tag{2.2}$$

We have taken the fluid to be isothermal far from the wall. This is an appropriate assumption for the Czochralski crystal growth technique. In this situation heat is supplied to the crucible only through the vertical sidewalls. Since the crucible stands on what is effectively an insulator all the incoming heat must exit through the upper surface of the melt, primarily by conduction through the growing crystal or radiation from the free surface of the melt. This results in a central core of the melt being of almost uniform temperature and so we consider a uniform temperature far from the wall. This is borne out by the recent calculations of Sackinger, Brown & Derby (1988).

In the standard boundary-layer solution of Pohlhausen (1921) for flow past a heated vertical wall with no magnetic field it is found that sufficiently far upstream the motions are almost parallel to the wall and the derivatives with respect to x are smaller than those with respect to y. If the terms that are relatively small are neglected we obtain the boundary-layer approximation in which the pressure is uniform everywhere, and that the flow and temperature are described by the set of equations

$$u\frac{\partial u}{\partial x}+v\frac{\partial u}{\partial y} = g\alpha(T-T_\infty)+\nu\frac{\partial^2 u}{\partial y^2},\quad \frac{\partial u}{\partial x}+\frac{\partial v}{\partial y} = 0,\quad u\frac{\partial T}{\partial x}+v\frac{\partial T}{\partial y} = \kappa\frac{\partial^2 T}{\partial y^2}. \qquad (2.3a\text{–}c)$$

These equations have a similarity solution of the form

$$u = \frac{\partial \psi}{\partial y},\quad v = -\frac{\partial \psi}{\partial x}, \qquad (2.4)$$

where

$$\psi = A_0 x^{\frac{3}{4}} f_0(\eta),\quad T = T_\infty + \Delta T g_0(\eta), \qquad (2.5)$$

and

$$\eta = \frac{y}{x^{\frac{1}{4}}\eta_0}. \qquad (2.6)$$

The constants A_0 and η_0 are given by

$$A_0 = (\nu^2 g\alpha\,\Delta T)^{\frac{1}{4}},\quad \eta_0 = \left(\frac{\nu^2}{g\alpha\,\Delta T}\right)^{\frac{1}{4}}. \qquad (2.7a, b)$$

This reduces the governing equations (3) to the pair of ordinary differential equations

$$\tfrac{1}{2}f_0' f_0' - \tfrac{3}{4}f_0'' f_0 = g_0 + f_0''',\quad -\tfrac{3}{4}f_0 g_0' = Pr^{-1} g_0'', \qquad (2.8a, b)$$

where the Prandtl number $Pr = \nu/\kappa$. The boundary conditions for this problem are

$$\left.\begin{aligned} &f_0(0) = f_0'(0) = 0,\quad g_0(0) = 1,\\ \text{and}\quad &g_0 \to 0,\quad f_0' \to 0 \quad \text{as} \quad \eta \to \infty. \end{aligned}\right\} \qquad (2.9)$$

The solution of these equations has $f_0 \sim a_0$ as $\eta \to \infty$, where a_0 is a constant dependent on the Prandtl number. This represents the entrainment of fluid that is required to replace the fluid rising in the heated boundary layer adjacent to the plate.

The boundary-layer approximation assumes that the flow is almost parallel to the vertical wall. Since the magnetic field, through the Lorenz force, only affects fluid flow across the magnetic field lines, this implies that there will be a weak direct interaction between the vertical magnetic field and the flow in the boundary layer. However, as noted above, the classical boundary-layer solution has, for large distances from the wall, a component of velocity towards the wall proportional to $x^{-\frac{1}{4}}$. If this boundary-layer solution holds in the case of the weak magnetic field then the full y-momentum equation, (2.1*b*), gives that for large distances from the wall

$$0 \approx \frac{1}{\rho}\frac{\partial p}{\partial y} - \frac{3\sigma B^2}{4\rho}A_0 x^{-\frac{1}{4}} f(\infty). \qquad (2.10)$$

Then assuming the pressure at the wall is uniform, we find

$$p(x,y) \propto y x^{-\frac{1}{4}}. \qquad (2.11)$$

This implies that the pressure gradients become unbounded far away from the wall. This result is not physically possible and so the presence of a vertical magnetic field will disrupt the far-field flow.

To find how the far-field flow adapts to a vertical field we assume that the vertical magnetic field is weak. The precise meaning of weak in this context will be quantified at the end of §4. If this is the case then the alteration to the flow far away from the wall will have a correspondingly weak effect on the flow near the wall, which will still be predominantly a balance between the buoyancy forces and viscosity. The weak magnetic field will provide a regular perturbation upon the flow near the wall. This perturbation will be determined by the flow far from the wall in the region where the magnetic field is important. This distance of this region from the wall will also be quantified in §3.

The procedure we follow here is to find an asymptotic expansion for the flow and temperature near the wall in terms of a small parameter representing the strength of the weak magnetic field; this is done in §3. We shall refer to this as the inner layer. Next, in §4, the motions far from the wall (in what we shall henceforth refer to as the outer layer) are found and matched to the inner layer. In §5 this far-field flow is used to provide the boundary conditions required to solve the higher-order equations in the inner layer. Finally the effect of viscosity on the outer layer will be considered in §6.

3. The inner layer

In the inner region the y-momentum equation (2.1b) gives, in the boundary-layer approximation, that

$$0 = -\frac{\partial p}{\partial y} - \sigma B^2 v. \tag{3.1}$$

For a sufficiently weak magnetic field the second term may be neglected and so in the inner layer the pressure is independent of y. However, we can no longer assume that outside this inner layer the pressure is also independent of x. Hence the boundary layer equations for the inner layer are

$$u\frac{\partial u}{\partial x} + v\frac{\partial u}{\partial y} = -\frac{1}{\rho}\frac{\mathrm{d}p(x)}{\mathrm{d}x} + g\alpha(T - T_\infty) + \nu\frac{\partial^2 u}{\partial y^2}, \tag{3.2a}$$

$$\frac{\partial u}{\partial x} + \frac{\partial v}{\partial y} = 0, \quad u\frac{\partial T}{\partial x} + v\frac{\partial T}{\partial y} = \kappa\frac{\partial^2 T}{\partial y^2}. \tag{3.2b, c}$$

We assume that the pressure term in (3.2a) is small and so the balances between the principal terms gives that the classical boundary-layer solution will provide the first approximation to the solution. Thus the stream function and temperature are approximated by

$$\psi \approx A_0 x^{\frac{3}{4}} f_0(\eta), \quad T \approx T_\infty + \Delta T g_0(\eta), \tag{3.3a, b}$$

where f_0 and g_0 denote the classical boundary-layer solution. We note that

$$f_0'(\eta) \to 0, \quad g_0(\eta) \to 0 \quad \text{as} \quad \eta \to \infty. \tag{3.4}$$

In order to further develop the solution in the inner layer we now briefly consider the situation in the outer layer. The expression (3.4) provides matching conditions for the outer layer and imply that it is isothermal. They also show that there is an entrainment at the inner edge of the outer layer and in particular require that $\psi \propto x^{\frac{3}{4}}$ as $y \to 0$ in the outer layer. Just as in the case of the inner layer, the flow in the outer layer is almost parallel to the wall for sufficiently large x, and so the boundary-layer approximation that the derivatives with respect to x are negligible when compared to the derivatives with respect to y, and the assumption that $u \gg v$ also hold. Thus the governing equations for the outer layer are

$$u\frac{\partial u}{\partial x} + v\frac{\partial u}{\partial y} = -\frac{1}{\rho}\frac{\partial p}{\partial x} + \nu\frac{\partial^2 u}{\partial y^2}, \quad 0 = -\frac{1}{\rho}\frac{\partial p}{\partial y} - \frac{\sigma B^2}{\rho}v, \quad \frac{\partial u}{\partial x} + \frac{\partial v}{\partial y} = 0. \tag{3.5a–c}$$

We look for similarity solutions of the form

$$\psi = A_1 x^{\alpha} h\left(\frac{y}{x^{\beta}\zeta_0}\right), \tag{3.6}$$

where α, β, A_1 and ζ_0 are constants to be determined, and find that for large x the viscosity term becomes small compared to the inertial terms in the x-momentum equation and is neglected. The balance between the remaining terms and the entrainment condition of the inner layer require that

$$\alpha = \tfrac{3}{4}, \quad \beta = \tfrac{7}{12}. \tag{3.7}$$

Hence the appropriate similarity variable, denoted by ζ, is defined by

$$\zeta = \frac{y}{x^{\frac{7}{12}}\zeta_0}, \tag{3.8a}$$

where

$$\zeta_0 = \left(\frac{\rho A_1}{\sigma B^2}\right)^{\frac{1}{3}}. \tag{3.8b}$$

From this we find, by integrating the y-momentum equation, that the pressure at the wall, denoted by p_{wall}, is

$$\left.\begin{aligned} p_{\text{wall}} &= -\sigma B^2 \int_0^{\infty} \frac{\partial \psi}{\partial x}\,\mathrm{d}y = -p_0 x^{\frac{1}{3}}, \\ \text{where} \qquad p_0 &= \tfrac{4}{3}\sigma B^2 A_1 \zeta_0 \int_0^{\infty} h(\zeta)\,\mathrm{d}\zeta, \end{aligned}\right\} \tag{3.9}$$

and so p_{wall} is proportional to $x^{\frac{1}{3}}$. In the inner-layer equations (3.2) it is the x-derivative of the wall pressure that appears. This is balanced by the nonlinear inertia terms, suggesting a perturbation parameter ξ of the form

$$\xi = x^{-\frac{1}{3}}/\xi_0. \tag{3.10}$$

We have now determined the form of the perturbation representing the pressure gradient outside the inner layer and so are able to develop the asymptotic solution in the inner layer where we look for solutions of the form

$$\psi = A_0 x^{\frac{3}{4}} f(\eta, \xi), \quad T = T_{\infty} + \Delta T g(\eta, \xi), \tag{3.11a, b}$$

where

$$\eta_0 = \left(\frac{\nu^2}{g\alpha\,\Delta T}\right)^{\frac{1}{4}}, \quad A_0 = (\nu^2 g\alpha\,\Delta T)^{\frac{1}{4}}, \quad \xi_0 = \left(\frac{\rho A_0^2}{p_0 \eta_0^2}\right)^{\frac{1}{2}}. \tag{3.12}$$

The boundary-layer equations (3.2) then give the following partial differential equations for f and g:

$$\tfrac{1}{2}f_{\eta}^2 - \tfrac{3}{4}f_{\eta\eta} f - \tfrac{1}{3}\xi f_{\eta} f_{\eta\xi} + \tfrac{1}{3}\xi f_{\xi} f_{\eta\eta} = \tfrac{1}{3}\xi^2 + g + f_{\eta\eta\eta} \tag{3.13a}$$

and

$$-\tfrac{3}{4} f g_{\eta} - \tfrac{1}{3}\xi f_{\eta} g_{\xi} + \tfrac{1}{3}\xi f_{\xi} g_{\eta} = Pr^{-1} g_{\eta\eta}. \tag{3.13b}$$

From (3.8), (3.9) and (3.12) the value of ξ is proportional to $B^{\frac{2}{3}}$. We assume the magnetic field to be sufficiently weak that ξ is small. Thus we seek a solution in the limit $\xi \to 0$ and hence put

$$f(\eta, \xi) = f_0(\eta) + \xi f_1(\eta) + \xi^2 f_2(\eta) + O(\xi^3), \tag{3.14a}$$

$$g(\eta, \xi) = g_0(\eta) + \xi g_1(\eta) + \xi^2 g_2(\eta) + O(\xi^3), \tag{3.14b}$$

where f_0 and g_0 represent the standard boundary-layer solution. The boundary conditions at the wall, $\eta = 0$, are

$$f_i(0) = f_i'(0) = g_i(0) = 0 \quad \text{for} \quad i \geqslant 1, \tag{3.15}$$

and the far field boundary conditions for g_i are

$$g_i(\eta) \to 0 \quad \text{as} \quad \eta \to \infty \quad \text{for} \quad i \geqslant 1. \tag{3.16}$$

We also require that the f_i are well behaved as $\eta \to \infty$. The precise meaning of this will be clarified later in this section.

The expansions (3.14) are substituted into the boundary-layer equations (3.13). The $O(\xi^0)$ equations are the standard boundary-layer equations (2.8). The next two orders give the following pairs of equations:

$O(\xi^1)$

$$-\tfrac{5}{12}f_0''f_1 + \tfrac{2}{3}f_0'f_1' - \tfrac{3}{4}f_0 f_1'' = g_1 + f_1''', \tag{3.17a}$$

$$-\tfrac{1}{3}f_1' g_1 - \tfrac{3}{4}f_0 g_1' - \tfrac{5}{12}f_1 g_0' = Pr^{-1} g_1''; \tag{3.17b}$$

$O(\xi^2)$

$$-\tfrac{1}{12}f_0''f_2 + \tfrac{1}{3}f_0'f_2' - \tfrac{3}{4}f_0 f_2'' + \tfrac{1}{6}f_1'f_1' - \tfrac{5}{12}f_1''f_1 = \tfrac{1}{3} + g_2 + f_2''', \tag{3.18a}$$

$$-\tfrac{2}{3}f_0' g_2 - \tfrac{3}{4}f_0 g_2' - \tfrac{1}{3}f_1' g_1 - \tfrac{5}{12}f_1 g_1' - \tfrac{1}{12}f_2 g_0' = \mathrm{Pr}^{-1} g_2''. \tag{3.18b}$$

In each case $g_1 \to 0$ as $\eta \to \infty$ and so we examine these equations to find the large-η behaviour for each f_i.

The $O(\xi)$-equations (3.17) show that

$$-\tfrac{3}{4}f_0 f_1'' \sim f_1''' \quad \text{as} \quad \eta \to \infty. \tag{3.19}$$

This gives that

$$f_1 \sim b_1 \eta + a_1 \quad \text{as} \quad \eta \to \infty. \tag{3.20}$$

Similarly, the $O(\xi^2)$-equations (3.18) give

$$\tfrac{1}{2}f_1' f_1' - \tfrac{3}{4}f_0 f_2'' - \tfrac{1}{3}f_1' f_1' \sim \tfrac{1}{3} + f_2''' \quad \text{as} \quad \eta \to \infty, \tag{3.21}$$

and so

$$f_2 \sim \frac{1}{9a_0}(b_1^2 - 2)\,\eta^2 + b_2 \eta + a_2 \quad \text{as} \quad \eta \to \infty. \tag{3.22}$$

Thus

$$f \sim a_0 + b_1 \xi\eta + \frac{1}{9a_0}(b_1^2 - 2)(\xi\eta)^2 + \dots \quad \text{as} \quad \eta \to \infty. \tag{3.23}$$

In this expression terms of the form $\xi^p \eta^q$ with $p > q$ have been ignored since they are not important when matching with the leading outer-layer solution. We note that this expansion breaks down when $\eta\xi = O(1)$. From (2.6), (3.8) and (3.10) $\zeta = O(\xi\eta)$ and so we find that the asymptotic solution (3.23) breaks down on the lengthscale of the outer layer.

The ordinary differential equations (3.17) and (3.18) can be solved numerically using standard techniques. However the value of b_1 required for the far-field boundary conditions for f_1 and f_2 can only be found by matching the inner layer onto the outer layer. This, combined with the breakdown of the asymptotic solution (3.14) on the lengthscale of the outer layer, leads us to now consider the outer layer in more detail.

4. The outer layer

In the outer layer the stream function is represented by the similarity form (3.6) in which case we find that the effect of viscosity is negligible at leading order. We formalize this by seeking a solution of the form

$$h = h_0(\zeta) + \xi h_1(\zeta) + O(\xi^2) \quad \text{as} \quad \xi \to \infty, \tag{4.1}$$

in which case the governing equations (3.5) give

$$-\tfrac{5}{12} h_0' h_0'' - \tfrac{3}{4} h_0 h_0''' = \tfrac{3}{16} h_0 - \tfrac{7}{144} \zeta h_0' - \tfrac{49}{144} \zeta^2 h_0'', \tag{4.2}$$

at leading order.

The main function of the outer layer is to overcome the infinite pressure gradients that would otherwise arise in the inner layer. Thus h_0 has to decay sufficiently rapidly for the pressure difference across the outer layer to be finite. Hence from (3.9) we require that

$$\left| \int_0^\infty h_0(\zeta)\, \mathrm{d}\zeta \right| < \infty. \tag{4.3}$$

At the inner edge of the outer layer the solution must match with the lage-η form of the inner-layer solution. The large-η behaviour of the inner-layer stream function is given from (3.3) and (3.23) by

$$\psi = A_0 x^{\frac{3}{4}} \left(a_0 + b_1 \xi \eta + \frac{1}{9a_0} (b_1^2 - 2) \xi^2 \eta^2 + \ldots \right) \quad \text{as} \quad \eta \to \infty. \tag{4.4}$$

For the outer layer, the small-ζ behaviour is given by

$$\psi = A_1 x^{\frac{3}{4}} (h_0(0) + h_0'(0) \zeta + \tfrac{1}{2} h_0''(0) \zeta^2 + \ldots). \tag{4.5}$$

We note that from (2.7), (3.8) and (3.12) ξ, η and ζ are related by

$$\xi \eta = \left(\frac{4H}{3} \right)^{\frac{1}{2}} \frac{A_1}{A_0} \zeta, \tag{4.6a}$$

where

$$H = \int_0^\infty h(\zeta)\, \mathrm{d}\zeta. \tag{4.6b}$$

We can expand H as an asymptotic series in ξ to obtain

$$H = H_0 + \xi H_1 + \xi^2 H_2 + \ldots, \tag{4.7a}$$

where

$$H_i = \int_0^\infty h_i(\zeta)\, \mathrm{d}\zeta, \quad i = 0, 1, 2, \ldots. \tag{4.7b}$$

We now match the inner and outer layers up to $O(\xi^2 \eta^2)$ and find that

$$A_0 a_0 = A_1 h_0(0), \quad b_1 \left(\frac{4H_0}{3} \right)^{\frac{1}{2}} = h_0'(0), \tag{4.8a, b}$$

$$\frac{A_1}{9a_0 A_0} \left(\frac{4H_0}{3} \right) (b_1^2 - 2) = \tfrac{1}{2} h_0''(0). \tag{4.8c}$$

Equation (4.8a) determines the scaling of the stream function in the outer layer, and so without loss of generality is satisfied by $A_1 = a_0 A_0$ and $h_0(0) = 1$. However (4.8b) does not explicitly determine $h_0'(0)$ as b_1 is unknown at this stage. The final matching condition (4.8*c*) also involves b_1 and so may be combined with (4.8*b*) to give the following expression for h_0:

$$h_0'(0)^2 - \tfrac{9}{2}h_0''(0) = \frac{8}{3}\int_0^\infty h_0(\zeta)\,\mathrm{d}\zeta. \tag{4.9}$$

However this condition can also be obtained by integrating (4.2) over the interval $0 < \zeta < \infty$, and so this gives no new conditions for the outer-layer solution.

So far we have only matched to $O(\xi^2)$. To match any more terms the higher-order behaviour in both layers would also have to be included, particularly the viscosity in the outer layer. To leading order this is not important for the bulk flow in the outer layer. By matching up to $O(\xi^2\eta^2)$ we have ensured the continuity of both velocity components and vorticity between the inner and outer layers.

We now consider the behaviour of h_0 as $\zeta \to \infty$. Examination of (4.2) shows that either h_0 is unbounded as $\zeta \to \infty$ or $h_0(\zeta) \equiv 0$ for sufficiently large values of ζ. The former would imply an infinite velocity far away from the wall and so is unphysical. Although $h_0(\zeta) \equiv 0$ is a solution to (4.2) for all ζ, it does not satisfy the boundary condition $h_0(0) = 1$. However, the highest derivative of h_0 is the third-order term which is multiplied by h_0. This implies that as $h_0 \to 0$ the behaviour of h_0 will become more singular. This allows the possibility that h_0 becomes zero at some finite value of ζ, say ζ^*, and then remains identically zero for larger values of ζ. We now look for solutions such that $h_0 \equiv 0$ for $\zeta > \zeta^*$. Then $h_0(\zeta)$ remains to be determined on $0 < \zeta < \zeta^*$ along with the unknown position ζ^*. Thus we have a free boundary problem for $h_0(\zeta)$ and ζ^* which satisfies the third-order differential equation (4.2) and so we require four boundary conditions. We have so far only determined two, that $h_0(0) = 1$ and $h_0(\zeta^*) = 0$. The other two boundary conditions are found from consideration of the singular behaviour of h_0 in the neighbourhood of $\zeta = \zeta^*$. The third condition is found from a jump condition at $\zeta = \zeta^*$. To determine this (4.2) is integrated over the interval $[\zeta^* - \epsilon, \zeta^* + \epsilon]$ to obtain

$$\left[\tfrac{1}{6}(h_0')^2 - \tfrac{3}{4}h_0 h_0''\right]_{\zeta^*-\epsilon}^{\zeta^*+\epsilon} = -\frac{4}{9}\int_{\zeta^*-\epsilon}^{\zeta^*+\epsilon} h_0(\zeta)\,\mathrm{d}\zeta + \tfrac{91}{144}\left[\zeta h_0(\zeta)\right]_{\zeta^*-\epsilon}^{\zeta^*+\epsilon} - \tfrac{49}{144}\left[\zeta^2 h_0'(\zeta)\right]_{\zeta^*-\epsilon}^{\zeta^*+\epsilon}. \tag{4.10}$$

We now take the limit $\epsilon \to 0$, and noting that h_0 is continuous and $h_0(\zeta^* + \epsilon) = 0$, equation (4.10) gives

$$\tfrac{1}{6}(h_0'(\zeta^*-))^2 - \tfrac{3}{4}h_0(\zeta^*-)h_0''(\zeta^*-) = -\tfrac{49}{144}\zeta^{*2}\,h_0'(\zeta^*-). \tag{4.11}$$

The asymptotic form of h_0 near ζ^* is given in the Appendix. From this we find that in general $h_0''(\zeta^* - \epsilon) = O(\epsilon^{-\frac{7}{9}})$, which would imply that the vorticity is in general unbounded as $\zeta \to \zeta^*-$. However this analysis also indicates that there is also a solution for which h_0'' remains bounded. It is this behaviour, with bounded vorticity in the neighbourhood of ζ^*, that is imposed as the last boundary condition. The reason for imposing this condition will be addressed in more detail in §6. The free-boundary problem for $(h_0(\zeta), \zeta^*)$ is

$$-\tfrac{5}{12}h_0' h_0'' - \tfrac{3}{4}h_0 h_0''' = \tfrac{3}{16}h_0 - \tfrac{7}{144}\zeta h_0' - \tfrac{49}{144}\zeta^2 h_0'', \tag{4.12a}$$

with boundary conditions

$$h_0(0) = 1$$

and

$$h_0(\zeta^*) = 0, \quad h_0'(\zeta^*) = -\tfrac{49}{24}\zeta^{*2}, \quad h_0''(\zeta^*) = \tfrac{1}{12}\zeta^*. \tag{4.12b}$$

We have solved this numerically. Because of the singular nature of the solution near ζ^* it was not possible to integrate numerically the solution all the way to or from

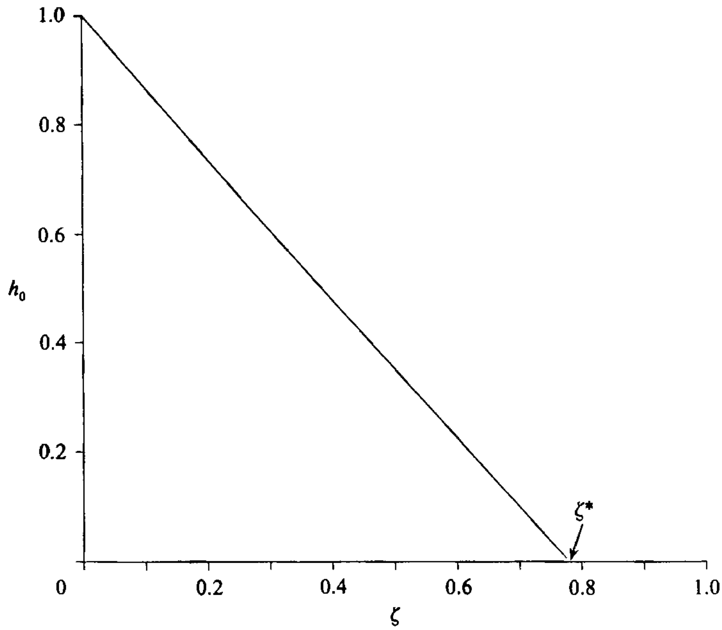

FIGURE 2. Graph of h_0 as a function of ζ. The curve meets the ζ-axis at ζ^* ($= 0.780290$) after which $h_0(\zeta) \equiv 0$.

the singular point. To overcome this problem the asymptotic form of the solution near ζ^* with h_0'' bounded was used. This enabled (4.2) to be integrated away from near the singular point. The solution is shown in figure 2.

The solution in the outer layer is composed of two distinct regions $[0, \zeta^*]$ and (ζ^*, ∞). In the latter region $h_0 \equiv 0$ and the fluid is stationary, we shall refer to it as the quiescent region. Thus the effect of the magnetic field is to cause the fluid to be entrained into the inner boundary layer only from a region close to the wall. The flow is confined as the magnetic field blocks fluid motion across the field lines in the far field. This contrasts with the situation in the absence of a magnetic field in which the boundary layer entrains fluid from the whole region. The whole flow is shown schematically in figure 3.

The solution $h_0(\zeta)$ has a discontinuity in its first derivative, and so the velocity of the fluid at $\zeta = \zeta^*$ is discontinuous. Thus a free shear layer will occur at $\zeta = \zeta^*$ near which viscosity will be important. This is considered in §6.

At this point we can now quantify the statement 'a weak magnetic field'. In the inner layer we require that ξ is small. There is also the requirement that the horizontal lengthscale of the outer layer is much larger than the horizontal lengthscale of the inner layer. From (4.6) these two requirements are equivalent. The value of ξ at a height x above the bottom edge of the sidewall is given by

$$\xi = \left(\frac{4H_0}{3}\right)^{\frac{1}{4}} \left(\frac{\sigma B^2 \nu f_0(\infty)^2}{\rho x g \alpha \Delta T}\right)^{\frac{1}{3}}, \tag{4.13}$$

where $H_0 = 0.3856$. The only remaining term in this expression that is not explicitly given or is a physical parameter is $f_0(\infty)$. This quantity is a function of the Prandtl number only.

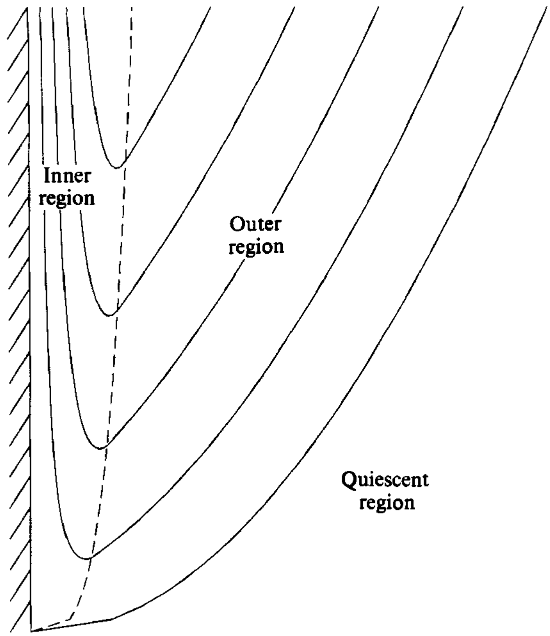

FIGURE 3. Schematic diagram of the flow showing the three regions; the inner layer, the outer layer, and the quiescent region.

5. The effect of the magnetic field on the inner layer

Having found the outer-layer solution we now have the boundary conditions for the perturbations f_1 and f_2 of the inner-layer solutions. From the matching condition (4.8*b*) between the inner and outer layers, and (3.20) and (3.22) we obtain

$$f_1'(\eta) \to \left(\frac{4H_0}{3}\right)^{-\frac{1}{2}} h_0'(0) \quad \text{as} \quad \eta \to \infty, \tag{5.1a}$$

and

$$f_2''(\eta) \to \frac{A_0}{A_1}\left(\frac{4H_0}{3}\right)^{-1} h_0''(0) \quad \text{as} \quad \eta \to \infty. \tag{5.1b}$$

This provides the remaining boundary condition for the differential equation (3.17). However (5.1*b*) is equivalent to the condition that $g_2 \to 0$ as $\eta \to \infty$. In order to obtain the extra boundary condition required to uniquely define f_2 and g_2 we need to find the higher-order behaviour of h. This higher-order behaviour includes the effect of viscosity and will be returned to in §6. We have solved (3.17) to obtain f_1 and g_1 using standard methods. Some results are shown in figure 4 for Prandtl numbers 0.01, 1.0 and 100.0. In the standard boundary-layer solution the temperature profile is the result of the balance between diffusion of heat away from the wall, and the advection of heat towards the wall by the entrained fluid. In each case the graph of $g_1(\eta)$ has an initial positive gradient. The graphs then rise to a peak and decay away in a similar fashion to g_0, but further away from the wall. Adding this to g_0 would have the effect of reducing the temperature gradient at the wall, and of increasing the depth of penetration of the heat from the wall. This is to be expected as the effect of the magnetic field is to oppose the entrainment. The graphs of f_1 are small near

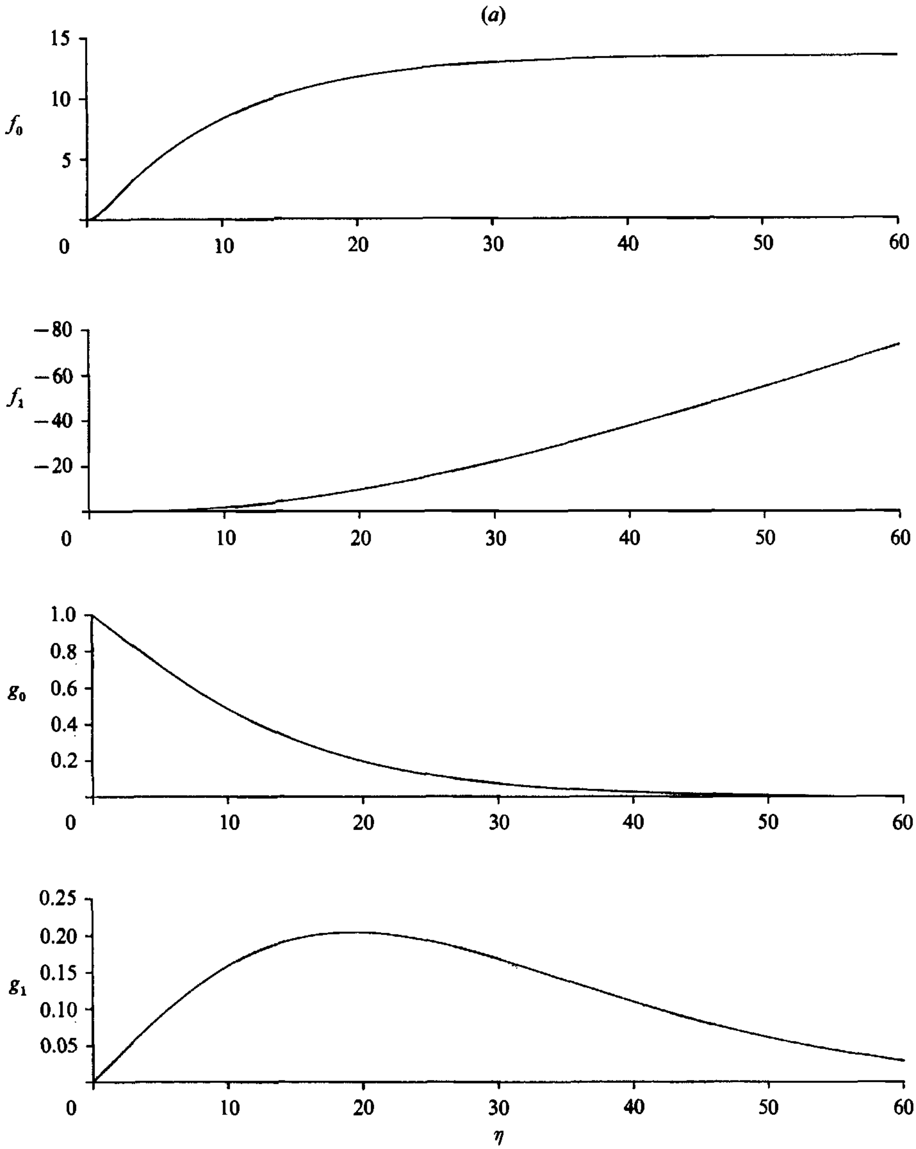

FIGURE 4(a). For caption see page 230.

the wall, gradually changing to the constant gradient required from the matching with the outer-layer solution.

Of interest in practical applications is the effect of the vertical magnetic field on the heat flux at the wall. We define the Nusselt number, Nu, to be the ratio of the total heat flux from a wall of a given height in the presence of a magnetic field to the heat flux when there is no magnetic field:

$$Nu = \int_0^L \frac{\partial T}{\partial y}\bigg|_{y=0} \mathrm{d}x \bigg/ \int_0^L \frac{\partial T}{\partial y}\bigg|_{y=0,\,B=0} \mathrm{d}x. \tag{5.2}$$

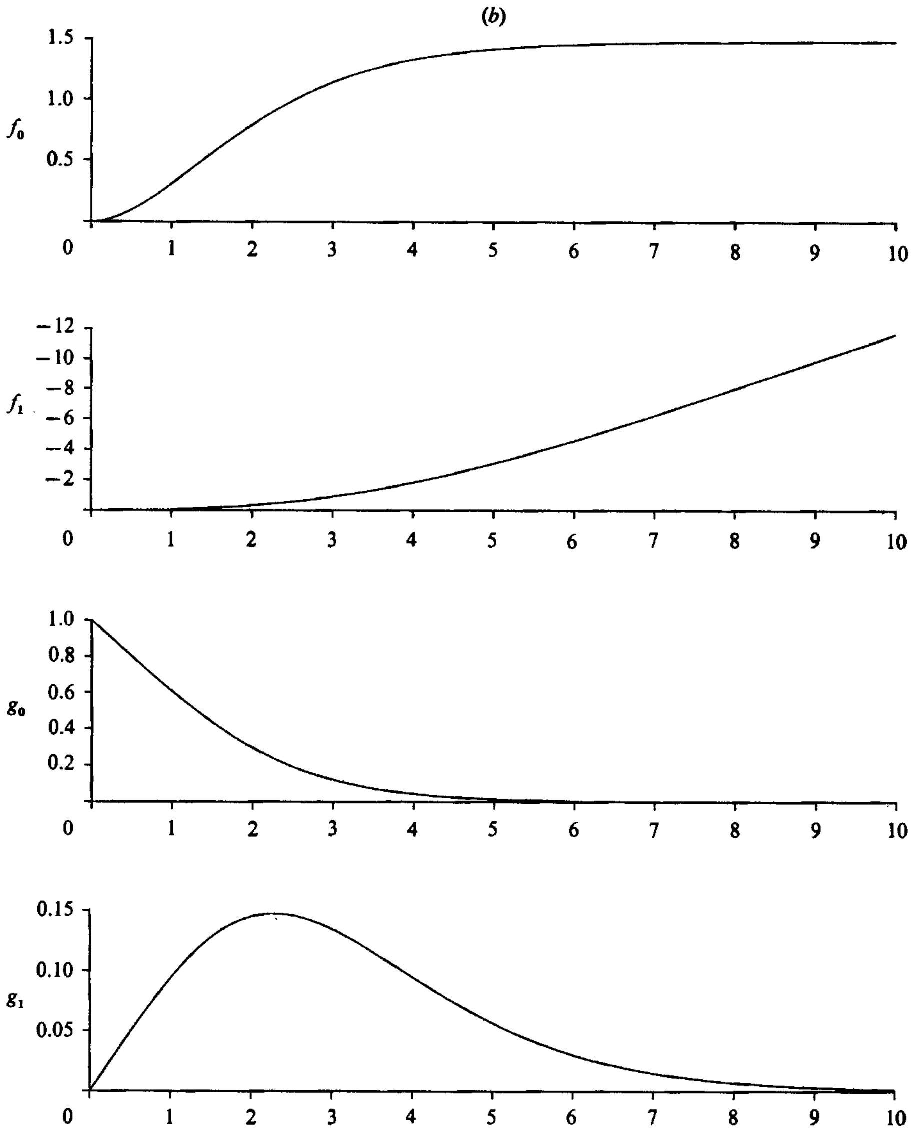

FIGURE 4 (*b*). For caption see page 230.

But from (3.14*b*), (2.6) and (3.10)

$$\left.\frac{\partial T}{\partial y}\right|_{y=0} = \Delta T\left(x^{-\frac{1}{4}}\frac{g_0'(0)}{\eta_0}+x^{-\frac{7}{12}}\frac{g_1'(0)}{\eta_0\,\xi_0}+\dots\right). \tag{5.3}$$

Hence, by integration with respect to x,

$$Nu = 1+\frac{9g_1'(0)}{5g_0'(0)}\,\xi_L+O(\xi_L^2), \tag{5.4}$$

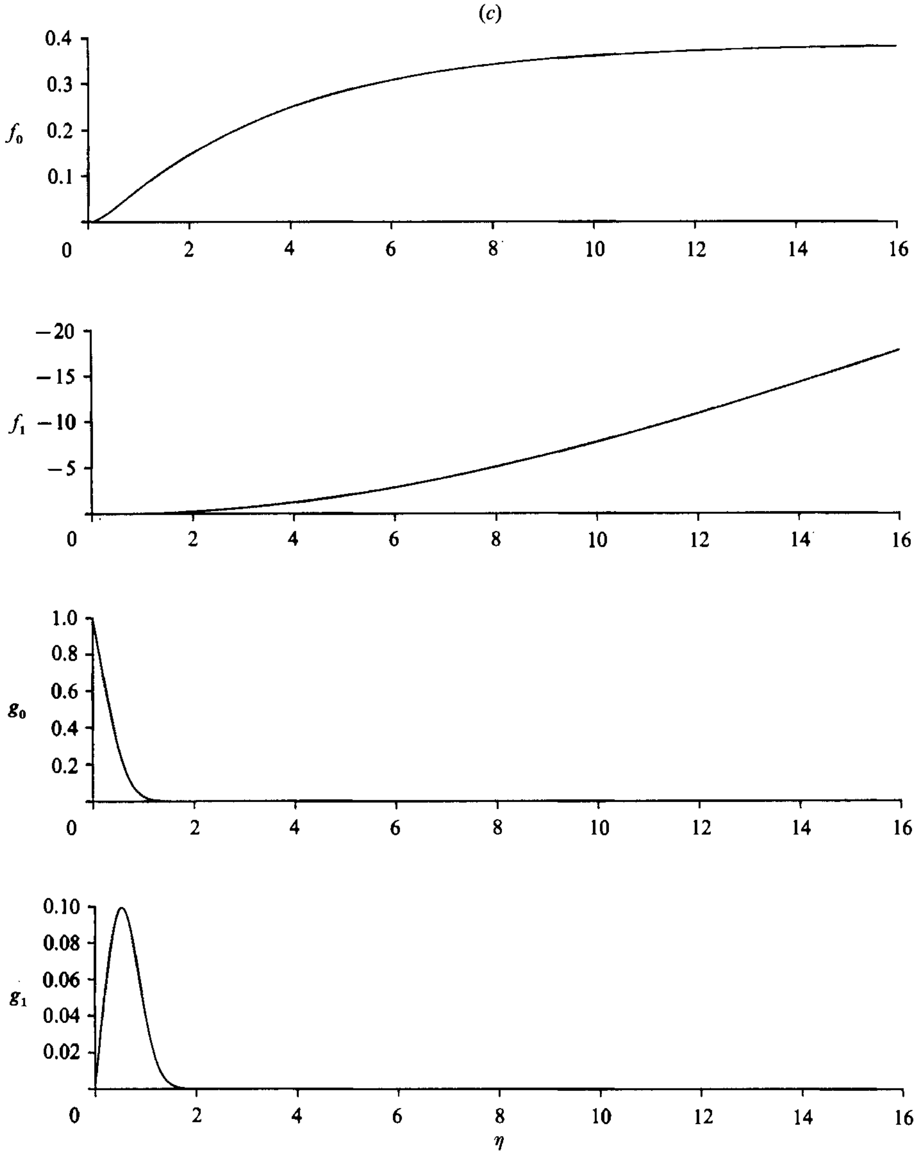

FIGURE 4. Graphs of f_0, f_1, g_0 and g_1 as functions of η for Prandtl numbers (*a*) 0.01, (*b*) 1.0, and (*c*) 100.0.

where ξ_L is ξ evaluated at the given height on the sidewall. The coefficient of ξ_L is shown graphically in figure 5 as a function of the Prandtl number. As is to be expected, the inhibiting effect of the magnetic field upon the flow reduces the heat flux and, hence, decreases the Nusselt number. This is seen by the negative coefficient of ξ.

From the definition of ξ, (4.13), there is a dependency on $f_0(\infty)$. This is the only quantity that is not a physical parameter of the system. The dependency of the perturbation to the Nusselt number on $f_0(\infty)$ can be removed by considering the Nusselt number expressed as a Taylor series in $\xi_L f_0(\infty)^{-\frac{2}{3}}$. The dependency of the first-order term in this series on the Prandtl number is shown in figure 6.

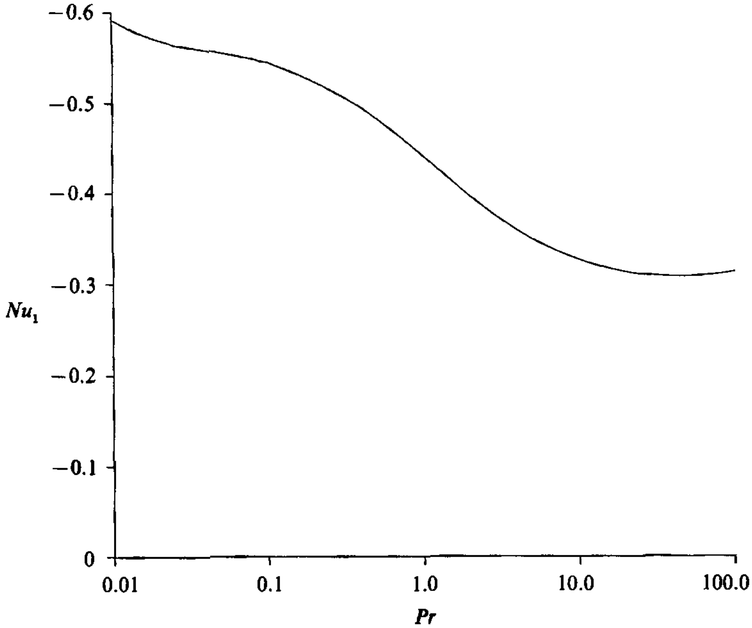

FIGURE 5. Graph of the leading-order perturbation to the Nusselt number, Nu_1, when the Nusselt number is expressed as a power series in ξ_L. Nu_1 is given for Prandtl numbers between 0.01 and 100.

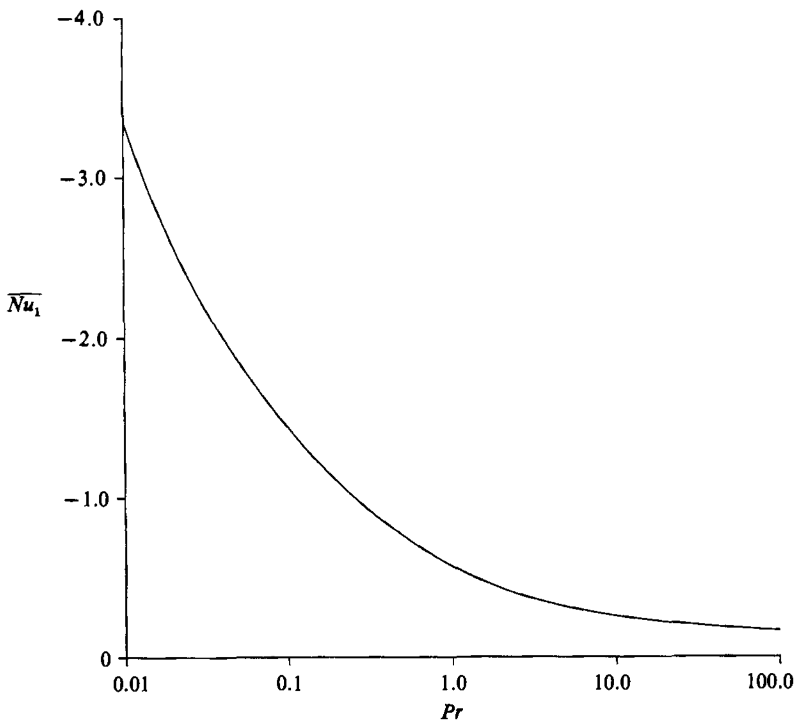

FIGURE 6. Graph of the leading-order perturbation to the Nusselt number, $\overline{Nu_1}$, when the Nusselt number is expressed as a power series in $\xi_L f_0(\infty)^{-\frac{4}{5}}$. This removes the dependency of the perturbation parameter on $f_0(\infty)$. $\overline{Nu_1}$ is given for Prandtl numbers between 0.01 and 100.

6. The effect of viscosity in the outer layer

In §4 a solution to the flow in the outer layer was found that had a discontinuity in the velocity away from the wall. This discontinuity represents a free shear layer. In the analysis that leads to this solution it was assumed that the effect of viscosity was negligible throughout the outer layer. However this will not be the case near the shear layer, and so we now look at this region in more detail.

The width of the outer layer is proportional to $x^{\frac{7}{12}}$ while the total downwards flux of fluid in this region is proportional to $x^{\frac{3}{4}}$, and so the average downwards velocity in the outer region is proportional to $x^{\frac{1}{6}}$. The velocity in this layer is almost uniform and so the jump in velocity at the free shear layer will also be proportional to $x^{\frac{1}{6}}$. Thus the downflow on the wall side of the free shear layer is decelerating, and will have streamlines that diverge from the shear layer. This precludes the possibility of a steady state that is similar to the form of the solution found in §4 occurring almost everywhere, except in a small region near the shear layer. This form could only be achieved if the diffusion of vorticity away from the shear layer is balanced by advection towards the shear layer, as in the case of stagnation-point flow towards a rigid wall (see, for example, Batchelor 1967). However, this is not the case here, and the effect of the viscosity may well be apparent throughout the outer layer. This problem arises because of the infinite extent of the fluid under consideration. In practical applications the heated surface is finite in length. In which case, depending on the situation at the top of the heated surface, there may be a mechanism that allows the possibility of a downflow that is of the kind found in §4. If this is the case then the effect of viscosity will again be negligible in all but the immediate vicinity of the free shear layer. In this section we shall consider how the flow near the shear layer would evolve in such a situation.

We seek a solution to (3.5) where the stream function is of the form

$$\psi = A_1 x^{\frac{3}{4}} h(\zeta, \bar{\xi}), \tag{6.1}$$

where ζ is as before and $\bar{\xi}$ is defined by

$$\bar{\xi} = x^{-\frac{1}{3}}/\xi_1 \quad \text{with} \quad \xi_1 = \left(\frac{\nu}{A_1 \zeta_0}\right)^{\frac{1}{2}}. \tag{6.2a, b}$$

This definition of $\bar{\xi}$ differs from that of ξ by a factor of $(\frac{4}{3}H)^{\frac{1}{2}}$. This leads to some simplification in the consideration of the shear layer.

When (6.1) is substituted into the governing equations (3.5) we obtain

$$-\tfrac{5}{12}h_\zeta h_{\zeta\zeta} - \tfrac{3}{4}h_{\zeta\zeta\zeta} h - \tfrac{1}{3}\bar{\xi}(h_\zeta h_{\bar{\xi}\zeta\zeta} - h_{\bar{\xi}} h_{\zeta\zeta\zeta})$$
$$= \tfrac{3}{16}h - \tfrac{7}{144}\zeta h_\zeta - \tfrac{49}{144}\zeta^2 h_{\zeta\zeta} + \tfrac{1}{18}\bar{\xi} h_{\bar{\xi}} - \tfrac{2}{3}\zeta\bar{\xi} h_{\zeta\bar{\xi}} - \tfrac{1}{9}\bar{\xi}^2 h_{\bar{\xi}\bar{\xi}} + \bar{\xi} h_{\zeta\zeta\zeta\zeta}. \tag{6.3}$$

We are concerned here with the case where the outer-layer solution, $h_0(\zeta)$, is imposed at some level up the wall where $\bar{\xi}$ is small, say $\bar{\xi}^*$. It is convenient to change variables so that $\bar{\xi}$ is replaced by θ, where

$$\bar{\xi} = e^\theta, \tag{6.4}$$

In this case (6.3) becomes

$$-\tfrac{5}{12}h_\zeta h_{\zeta\zeta} - \tfrac{3}{4}h_{\zeta\zeta\zeta} h - \tfrac{1}{3}(h_\zeta h_{\theta\zeta\zeta} - h_\theta h_{\zeta\zeta\zeta})$$
$$= \tfrac{3}{16}h - \tfrac{7}{144}\zeta h_\zeta - \tfrac{49}{144}\zeta^2 h_{\zeta\zeta} + \tfrac{1}{18}h_\theta - \tfrac{2}{3}\zeta h_{\zeta\theta} - \tfrac{1}{9}h_{\theta\theta} + e^\theta h_{\zeta\zeta\zeta\zeta}, \tag{6.5}$$

with the inviscid free solution, $h_0(\zeta)$, imposed at $\theta = \theta^*$ $(= \log_e \bar{\xi}^*)$. We now look at the evolution of the flow in the region near the level of the shear-layer solution by rescaling ζ and h to give

$$e^{\frac{1}{2}\theta^*}\chi = \zeta - \zeta^*, \quad e^{\frac{1}{2}\theta^*}h^* = h, \tag{6.6}$$

where ξ^* is the location of the shear layer. If these are substituted into (6.5) and all but the lowest-order terms are ignored, the governing equation for the evolution of the shear layer is

$$-\tfrac{5}{12}h^*_\chi h^*_{\chi\chi} - \tfrac{3}{4}h^*_{\chi\chi\chi}h^* - \tfrac{1}{3}(h^*_\chi h^*_{\theta\chi\chi} - h^*_\theta h^*_{\chi\chi\chi}) = -\tfrac{49}{144}\zeta^{*2}h^*_{\chi\chi} + e^{\theta-\theta^*}h^*_{\chi\chi\chi\chi}. \tag{6.7}$$

For solutions near $\theta = \theta^*$ we assume that $e^{\theta-\theta^*} \approx 1$. Equation (6.7) can be integrated once with respect to χ to give

$$\tfrac{1}{6}h^*_\chi h^*_\chi - \tfrac{3}{4}h^*_{\chi\chi}h^* - \tfrac{1}{3}(h^*_\chi h^*_{\theta\chi} - h^*_\theta h^*_{\chi\chi}) = -\tfrac{49}{144}\zeta^{*2}h^*_\chi + h^*_{\chi\chi\chi} + D(\theta), \tag{6.8}$$

where $D(\theta)$ is an arbitrary function of θ. The boundary conditions on h^* for large $|\chi|$ are

$$h^* \to 0 \quad \text{as} \quad \chi \to \infty, \tag{6.9a}$$

and

$$h^* \sim -\tfrac{49}{24}\zeta^{*2}\chi + o(1) \quad \text{as} \quad \chi \to -\infty. \tag{6.9b}$$

The $o(1)$-term in the second boundary condition (6.9*b*) is required in order to locate the solution at the origin as (6.8) is translationally invariant with respect to χ. Both of these conditions require that $D(\theta) \equiv 0$. For solutions to (6.8) that are valid for small $\theta - \theta^*$ we can find a similarity solution of the form

$$h^* = (\theta-\theta^*)^{\frac{1}{2}}k(\varphi), \quad \text{where} \quad \varphi = \frac{\chi}{(\theta-\theta^*)^{\frac{1}{2}}}. \tag{6.10}$$

If we expand k as an asymptotic series in $(\theta-\theta^*)^{\frac{1}{2}}$ and substitute the series into (6.8) we obtain the leading-order equation for k_0

$$k_0''' = \tfrac{1}{6}k_0''k_0, \tag{6.11}$$

with boundary conditions

$$\left.\begin{aligned} k_0 &\to -\tfrac{49}{24}\zeta^{*2}\varphi + o(1) \quad \text{as} \quad \varphi \to -\infty, \\ \text{and} \qquad k_0 &\to 0 \quad \text{as} \quad \varphi \to \infty. \end{aligned}\right\} \tag{6.12}$$

The solution to this is shown in figure 7. It can be shown that k_0 approaches the linear asymptote super-exponentially for large negative φ and that k_0 approaches zero as $-18\,\varphi^{-1}$ for large positive φ. These features are reflected in figure 7.

The next-order equation for $k_1(\varphi)$ allows solutions that, for large negative values of φ, behave as

$$k_1(\varphi) \sim A\varphi^2 + B. \tag{6.13}$$

This behaviour can only be matched onto the asymptotic form of h_0 near to ζ^* if h_0'' remains bounded. For this reason the condition that the vorticity remains bounded in the limit $\zeta \to \zeta^*-$ was imposed in §4.

A similar approach to the examination of the shear layer can be applied to the investigation of higher-order approximations to $h(\zeta)$. Because of the lack of a global solution for h if viscosity is retained, a similar local approach must again be used. However the results yielded will be dependent on the particular situation at the top of the wall. This cannot be treated in a general way and so is outside the scope of this paper.

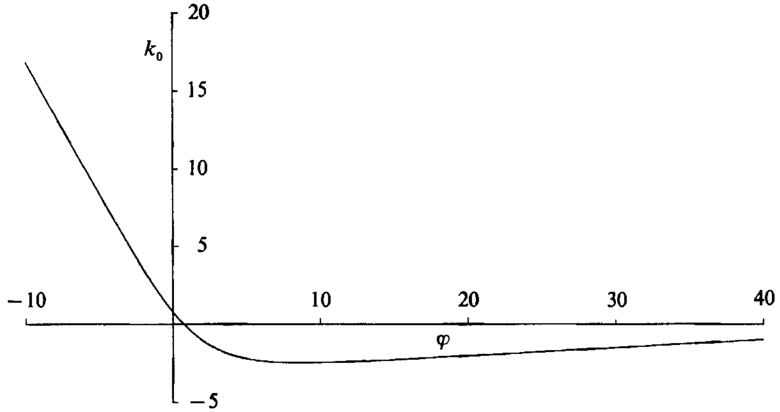

FIGURE 7. Graph of k_0 against φ, showing the form of the similarity solution for the spatial evolution of the shear layer in the presence of viscosity.

7. Conclusions

In this paper we have investigated how a weak vertical magnetic field interacts with a boundary-layer flow past a heated vertical wall. We have shown that the effect of the magnetic field is to inhibit the entrainment of fluid into the boundary layer from regions far from the wall, but instead limits the entrainment to a region of thickness proportional to $B^{-\frac{2}{3}}$. The similarity solution found for this outer layer involves a free shear layer. This causes the assumption that the outer layer is effectively inviscid to break down in the neighbourhood of the shear layer. This breakdown is important globally if the fluid region is infinite; however if the fluid is finite in extent, and the model is applied to a finite region then the leading-order behaviour found in this paper is appropriate. Higher-order behaviour would have to be investigated in the context of the particular physical situation under consideration and cannot be addressed by the general approach adopted here.

This work has been motivated by the desire to understand some of the details of the melt motion in the Czochralski crystal growing technique, albeit through the study of a much simplified model. Unfortunately we can offer no experimental comparison for the work presented here. For the Czochralski crystal growth system the assumption of a uniform temperature T_∞ may be justfied; however in the experimental work of Seki *et al.* (1979) it may not be appropriate. Their experiments consisted of a rectangular cavity with a cooled vertical wall opposite the heated wall. Hence it is likely that the interior of the fluid will be thermally stratified (cf. Gill 1966) and our theory is not strictly appropriate. However our work is more relevant to their experiments than that of Sparrow & Cess (1961) with which they compared their experimental results. In their analysis Sparrow & Cess considered a weak horizontal field rather than the vertical field employed in the experiments.

Finally we note that the solution presented here is valid only for large x, in the same way as the Pohlhausen boundary-layer solution. For parameters relevant to the Czochralski growth of silicon the two-region structure described above breaks down on the same lengthscale as the Pohlhausen solution.

The first author would like to acknowledge the financial support of the Science and Engineering Research Council in this work.

Appendix. Solution to $h(\zeta)$ near ζ^*

To find the general solution of (4:2) near $\zeta = \zeta^*$ it is convenient to transform h and ζ to

$$\epsilon\bar{\zeta} = \zeta^* - \zeta, \quad \epsilon\bar{h} = h_0. \tag{A 1}$$

Then (4.2) becomes

$$\tfrac{5}{12}\bar{h}'\bar{h}'' + \tfrac{3}{4}h'''\bar{h} = \tfrac{3}{16}\epsilon^2\bar{h} + \tfrac{7}{144}\epsilon(\zeta^* - \epsilon\bar{\zeta})\,\bar{h}' - \tfrac{49}{144}(\zeta^* - \epsilon\bar{\zeta})^2\,\bar{h}''. \tag{A 2}$$

We now require that $\bar{h} \equiv 0$ for all $\bar{\zeta} > 0$. If we look for solutions near to the origin, ϵ small, we get the $O(1)$ equation for $\bar{h}$

$$\tfrac{5}{12}\bar{h}'\bar{h}'' + \tfrac{3}{4}\bar{h}'''\bar{h} = -\tfrac{49}{144}\zeta^{*2}\,h''. \tag{A 3}$$

This can be integrated once to give

$$-\tfrac{1}{6}\bar{h}'\bar{h}' + \tfrac{3}{4}h''\bar{h} = -\tfrac{49}{144}\zeta^{*2}\bar{h}' + A, \tag{A 4}$$

where A is a constant. However the jump condition (4.11), when rescaled, gives $A = 0$. We now multiply (A 4) by $\bar{h}^{-\frac{11}{9}}$ and integrate the equation once more to obtain

$$\bar{h}' = \tfrac{49}{24}\zeta^{*2} + C\bar{h}^{\frac{2}{9}}. \tag{A 5}$$

This can be integrated to give $\bar{\zeta}$ in terms of $\bar{h}$ for $\bar{h} > 0$ and $\bar{\zeta} > 0$; three cases arise

(i) $C > 0$

$$\bar{\zeta} = \frac{9D^{\frac{7}{9}}}{C}\left[\tan^{-1}\left(\left(\frac{\bar{h}}{D}\right)^{\frac{1}{9}}\right) - \left(\frac{\bar{h}}{D}\right)^{\frac{1}{9}} + \frac{1}{3}\left(\frac{\bar{h}}{D}\right)^{\frac{3}{9}} - \frac{1}{5}\left(\frac{\bar{h}}{D}\right)^{\frac{5}{9}} + \frac{1}{7}\left(\frac{\bar{h}}{D}\right)^{\frac{7}{9}}\right]; \tag{A 6a}$$

(ii) $C < 0$

$$\bar{\zeta} = \frac{9D^{\frac{7}{9}}}{|C|}\left[\tanh^{-1}\left(\left(\frac{\bar{h}}{d}\right)^{\frac{1}{9}}\right) - \left(\frac{\bar{h}}{D}\right)^{\frac{1}{9}} - \frac{1}{3}\left(\frac{\bar{h}}{D}\right)^{\frac{3}{9}} - \frac{1}{5}\left(\frac{\bar{h}}{D}\right)^{\frac{5}{9}} - \frac{1}{7}\left(\frac{\bar{h}}{D}\right)^{\frac{7}{9}}\right], \tag{A 6b}$$

where

$$|C|D^{\frac{2}{9}} = \tfrac{49}{24}\zeta^{*2}; \tag{A 6c}$$

(iii) $C = 0$

$$\bar{h}(\bar{\zeta}) = \tfrac{49}{24}\zeta^{*2}\bar{\zeta}. \tag{A 7}$$

In both the cases with $C \neq 0$, $\bar{h}''(\bar{\zeta}) = O(\bar{\zeta}^{-\frac{7}{9}})$ as $\bar{\zeta} \to 0+$. The last case, $C = 0$, can be found more accurately by looking for a power-series solution of the form

$$\bar{h}(\bar{\zeta}) = a\bar{\zeta} + \epsilon b\bar{\zeta}^2 + \epsilon^2 c\bar{\zeta}^3 + \dots. \tag{A 8}$$

This is substituted into (A 2) and like powers of ϵ are equated. With the application of the jump condition, the first three coefficients are found to be

$$a = \frac{49}{24}\zeta^{*2}, \quad b = \frac{\zeta^*}{24}, \quad c = \frac{295}{14112}. \tag{A 9}$$

REFERENCES

BATCHELOR, G. K. 1967 *An Introduction to Fluid Dynamics.* Cambridge University Press.

GILL, A. E. 1966 The boundary-layer regime for convection in a rectangular cavity. *J. Fluid Mech.* **26**, 515.

GRAY, D. D. 1977 Laminar plume above a line heat source in a transverse magnetic field. *Appl. Sci. Res.* **33**, 437.

HJELLMING, L. N. & WALKER, J. S. 1987 Melt motion in Czochralski crystal puller with an axial magnetic field: motion due to buoyancy and thermocapillarity. *J. Fluid Mech.* **182**, 335.

LYKOUDIS, P. S. 1962 Natural convection of an electrically conducting fluid in the presence of a magnetic field. *Intl J. Heat Mass Transfer* **5**, 23.

POHLHAUSEN, E. 1921 Der Wärmeaustausch zwischen festen Körpen Flüssigkeiten mit kleiner Reibung und kleiner Wärmeleitung. *Z. angew. Math. Mech.* **1**, 115.

RILEY, N. 1976 A note on 'simplfication and scaling'. *Proc. Edinburgh Math. Soc.* **20**, 63.

SACKINGER, P. A., BROWN, R. A. & DERBY, J. J. 1988 Finite element method for analysis of fluid flow, heat transfer and free interfaces in Czochralski crystal growth. *Intl J. Num. Meth. Fluids* (submitted).

SEKI, M., KAWAMURA, H. & SANOKAWA, K. 1979 Natural convection of mercury in a magnetic field parallel to the gravity. *Trans. ASME* C: *J. Heat Transfer* **101**, 227.

SOWARD, A. M. 1969 Steady free convection above a point heat source and a horizontal line heat source in a vertical magnetic field. *J. Fluid Mech.* **39**, 753.

SPARROW, E. M. & CESS, R. D. 1961 The effect of a magnetic field on free convection heat transfer. *Intl J. Heat Transfer* **3**, 267.

WILKS, G. 1976 Magnetohydrodynamic free convection about a semi-infinite vertical plate in a strong cross field. *Z. angew. Math. Phys.* **27**, 621.